

Structural and magnetic properties of $\text{Sr}_2\text{Fe}_{1+x}\text{Mo}_{1-x}\text{O}_6$ ($-1 \leq x \leq 0.25$)

Dinesh Topwal,¹ D. D. Sarma,^{1,*} H. Kato,^{2,†} Y. Tokura,^{2,3} and M. Avignon⁴

¹*Solid State and Structural Chemistry Unit, Indian Institute of Science, Bangalore 560012, India*

²*Correlated Electron Research Center, AIST, Tsukuba 305-8562, Japan*

³*Department of Applied Physics, University of Tokyo, Tokyo 113-8656, Japan*

⁴*Laboratoire d'Etudes des Propriétés Electroniques des Solides, CNRS, BP 166, 38042 Grenoble Cedex 9, France*

(Received 3 November 2005; revised manuscript received 18 January 2006; published 17 March 2006)

We have synthesized the solid solution $\text{Sr}_2\text{Fe}_{1+x}\text{Mo}_{1-x}\text{O}_6$ with $-1 \leq x \leq 0.25$, the composition $x=0$ corresponding to the well-known double-perovskite system $\text{Sr}_2\text{FeMoO}_6$. We report structural and magnetic properties of the above system, exhibiting systematic variations across the series. These results restrict the range of models that can explain magnetism in this family of compounds, providing an understanding of the magnetic structure.

DOI: [10.1103/PhysRevB.73.094419](https://doi.org/10.1103/PhysRevB.73.094419)

PACS number(s): 75.30.-m, 72.15.Eb, 71.27.+a, 75.25.+z

I. INTRODUCTION

Half-metallic ferromagnetic oxides¹ have attracted extensive attention not only as a source of fully polarized charge carriers for spintronics applications, but also as potential candidates for memory devices by the virtue of their large magnetoresistance (MR). Recently, a double perovskite $\text{Sr}_2\text{FeMoO}_6$, belonging to this general family of half-metallic ferromagnetic oxides, has shown spectacularly large MR even at the room temperature and at relatively small applied magnetic fields² compared to the extensively investigated class of magnetoresistive manganites, due to a substantially enhanced Curie temperature (T_c). The enhanced T_c and the origin of ferromagnetism in $\text{Sr}_2\text{FeMoO}_6$ and related compounds have been explained³ in terms of a kinetically driven mechanism. It is interesting to note that the same mechanism was later invoked⁴⁻⁶ to explain ferromagnetism in the recently discovered dilute magnetic semiconductors (DMS's), such as Mn-doped GaAs, thereby connecting two apparently disparate classes of compounds.

A perfectly ordered lattice of $\text{Sr}_2\text{FeMoO}_6$ consists of alternating FeO_6 and MoO_6 octahedra along all the three cubic axes of the perovskite structure. It is believed that the fully ordered compound is a half-metallic ferromagnet with *nominal* ionic configurations of Fe^{3+} and Mo^{5+} . The measured value of the saturation magnetization M_s in normally prepared samples is invariably found^{2,7,8} to be lower than the expected value of $4\mu_B$ per formula unit (f.u.) from the half-metallic state. This is due to the inevitable presence of mis-site disorders, where some Fe and Mo interchange their crystallographic positions. However, the microscopic origin of the reduction in M_s is still not entirely clear. Both classical Monte Carlo simulations⁹ and quantum-mechanical band-structure calculations¹⁰ indeed predicted a reduction of M_s as a function of mis-site disorder, but the underlying reasons for this reduction are very different in these two proposals. In one case,⁹ it is assumed that the moment reduction is only due to antiferromagnetically coupled Fe pairs whenever Fe-O-Fe bonds are generated by such mis-site disorders. In this view, the conduction band presumably retains its polarization to a large extent. In contrast, the band-structure approach¹⁰

attributed the reduction of the moment to strong depolarization effects at each site, though all Fe sites were found to be ferromagnetically coupled. The mis-site disorder and its effect on the conduction band are not only important in the context of spin-injection devices; the magnetoresistive properties of these samples also appear to be strongly influenced by these factors.^{11,12} Therefore, it is important to investigate experimentally the underlying details of the magnetic structure and the effect of mis-site disorder to obtain a definitive understanding of magnetism in this class of compounds.

There have been some efforts to study samples with different extents of disorder;^{11,13-16} however, in view of the difficulty to have a microscopic and detailed control of such a statistical process, we have adopted a different route to probe issues raised here. We have prepared $\text{Sr}_2\text{Fe}_{1+x}\text{Mo}_{1-x}\text{O}_6$ over a wide range of compositions ($-1 \leq x \leq 0.25$). The ideal $x=0$ composition corresponds to the maximal Fe content possible in this crystal structure, while avoiding a nearest-neighbor Fe-O-Fe arrangement. Therefore, in the Fe-deficient regime ($x < 0$) we control the average separation between the magnetic ions by changing x . In the Fe-rich composition ($x > 0$), we replace some of the Mo's with Fe in the ordered structure, thereby forcing the additional Fe ions necessarily to form Fe-O-Fe 180° bonds. Thus, we obtain a control on number of such bonds introduced in the system by controlling x . We report here a detailed investigation of transport and magnetic properties of this family of compounds. Our results conclusively show that while the Fe-O-Fe bond is indeed antiferromagnetically coupled, the conduction bands in these system are also far from being 100% polarized. Interestingly, this system shows a rapid increase of T_c with increasing x until approximately $x=0$, followed by a near saturation.

II. EXPERIMENT

Polycrystalline samples of $\text{Sr}_2\text{Fe}_{1+x}\text{Mo}_{1-x}\text{O}_6$ for $x > 0$ were prepared by melting a stoichiometric mixture of SrCO_3 , Fe_2O_3 , MoO_3 , and Mo in an inert gas (Ar) arc furnace.¹³ The obtained ingots were crushed and made into pellets. These pellets were sintered at 1250 °C in a reducing atmosphere consisting of 1% H_2 and 99% Ar flow for 16 h to achieve the

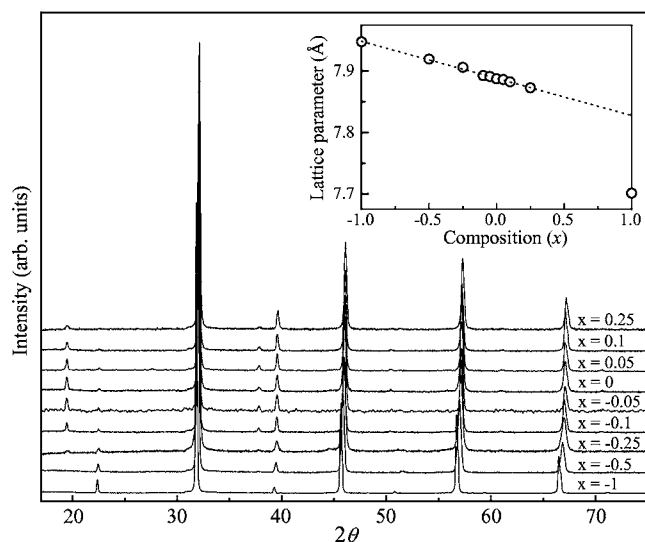


FIG. 1. X-ray powder diffraction patterns of $\text{Sr}_2\text{Fe}_{1+x}\text{Mo}_{1-x}\text{O}_6$ using $\text{Cu } K\alpha$ radiation. The apparent shoulder, most clearly visible for the diffraction peak at $\Theta \approx 67^\circ$ for the $x = -1$ composition, arises from the $\text{Cu } K\alpha_2$ contribution. The inset shows the variation of lattice parameter a as a function of the composition. The data for $x = 1$ corresponding to SrFeO_3 are taken from Ref. 17.

maximum ordering between Fe and Mo and to remove a small amount ($< 2\%$) of SrMoO_4 present at times. The samples with lower Fe concentrations ($x \leq 0$) were made by the normal solid-state synthesis.² In this case, the stoichiometric mixture of SrCO_3 , Fe_2O_3 , and MoO_3 was first heated in air at 900°C for 3 h, followed by a reaction in the pellet form at 1250°C for 10 h. in a mixture of Ar and H_2 and then furnace cooled in the flow of the same reducing gas mixture. The above process of heating in the reducing atmosphere was repeated 2–3 times with intermediate grindings to ensure a homogeneous, pure phase. The ratio of H_2 :Ar varied from 15:85 for the $x = -1$ sample to 2:98 for the $x = 0$ sample. X-ray powder diffraction measurements established the formation of a single-phase material in every case. We also used energy dispersive analysis of x-rays (EDAX) in conjunction with secondary electron microscopy (SEM) extensively, to obtain the concentration ratio between Fe and Mo in different grains as well as at several points within the same grain for each sample in order to establish the homogeneity of the samples. The magnetic properties of the sample were measured using Quantum Design's Magnetic Properties Measurement System (MPMS)

III. RESULTS AND DISCUSSION

Figure 1 shows the powder x-ray diffraction patterns for various compositions of $\text{Sr}_2\text{Fe}_{1+x}\text{Mo}_{1-x}\text{O}_6$. It is well known¹³ that the more intense supercell reflection peaks corresponding to the double-perovskite structure appear at $2\theta = 19.4^\circ$ and 37.8° in $\text{Sr}_2\text{FeMoO}_6$. Both these diffraction peaks gradually lose intensity with a deviation of x from 0, as seen in Fig. 1. The observation of these diffraction peaks over an extended range of compositions, $-0.25 \leq x \leq 0.25$, in $\text{Sr}_2\text{Fe}_{1+x}\text{Mo}_{1-x}\text{O}_6$ is interesting and suggests that Fe prefer-

entially occupies one sublattice and Mo the other one even for compositions away from the ideal Fe:Mo::1:1 composition. The x-ray diffraction pattern establishes a systematic reduction in the unit cell parameters, as evidenced by a monotonic shift of all diffraction peaks to higher angles with increasing x . We plot the variation of the lattice parameter a as obtained from Rietveld refinements as a function of composition x in the inset to Fig. 1. We have also shown from the literature¹⁷ the corresponding lattice parameter of SrFeO_3 which is one end member of this series, $\text{Sr}_2\text{Fe}_{1+x}\text{Mo}_{1-x}\text{O}_6$, with $x = 1$. It is interesting to note that the variation of a over the range of compositions ($-1 \leq x \leq 0.25$) studied here is linear with the composition x . However, the extrapolation of this linear trend to the $x = 1$ end point is in complete disagreement with the observed result for SrFeO_3 , suggesting a drastic or sudden change of valency between $x = 0.25$ and $x = 1$ consistent with the fact that Fe is in Fe^{4+} state in SrFeO_3 (i.e., $x = 1$) and in the Fe^{3+} state in $\text{Sr}_2\text{FeMoO}_6$ (i.e., $x = 0$). However, a substitution of Mo^{5+} by Fe^{3+} or *vice versa*, as in $\text{Sr}_2\text{Fe}_{1+x}\text{Mo}_{1-x}\text{O}_6$ with $x \neq 0$, cannot satisfy the charge neutrality without changing the valency of Mo, provided Fe remains in the trivalent state. Mo is known to adopt readily valence state between 4+ and 6+. Simple considerations then show that Fe can remain in the trivalent state for $-1 \leq x < 1/3$ with Mo continuously changing its valency from Mo^{6+} for $x = 1/3$ to Mo^{4+} for $x = -1$. This suggests that Fe cannot retain its trivalent state for $x \geq 1/3$, as Mo cannot take up a valency larger than 6+. Thus, it appears that a systematic and continuous change in the lattice parameters for $-1 \leq x \leq 0.25$ is due to the progressive replacement of Fe by Mo, retaining Fe in the trivalent state, while the discontinuous change in the lattice parameter for SrFeO_3 is due to the change of Fe valency. Recent Mössbauer studies¹⁸ of the solid solution over the relevant x range indeed support the existence of essentially the same charge state of Fe over this range of compositions, as evidenced by the isomer shifts and the hyperfine fields being 0.69 ± 0.04 mm/s and 479 ± 3 KOe, respectively for all the compositions reported here.

Figure 2 shows the dependence of resistivity on the temperature, $\rho(T)$. It is clear that all the samples show relatively less dependence on the temperature, with $\rho(T)$ exhibiting a maximum of a factor of 1.7 variation over the entire range of T . Moreover, most of the $\rho(T)$ plots clearly show a decreasing trend with decreasing T , at least in the high-temperature regime, suggesting a metallic state. The earlier reported resistivity¹⁹ in these samples shows semiconducting behavior for $x \geq 0.2$, which is also accompanied by a structural phase transition from tetragonal lattice to cubic lattice with increasing x . On the basis of the simple considerations presented above, we believe that it is not possible to make samples by the normal route beyond $x = 1/3$ as this would imply converting some Fe to the tetravalent state; such samples would instead tend to become oxygen deficient. This tendency to develop oxygen nonstoichiometry for higher Fe compositions may be responsible for the semiconducting behavior reported in Ref. 19. A few of the samples such as $x = 0.05$ and 0.0 exhibit a gently increasing behavior with decreasing T over the entire temperature range, where as a few others, such as $x = -0.25$, -0.05 , and 0.25, show an upturn of resistivity only at a lower temperature. This increasing trend of

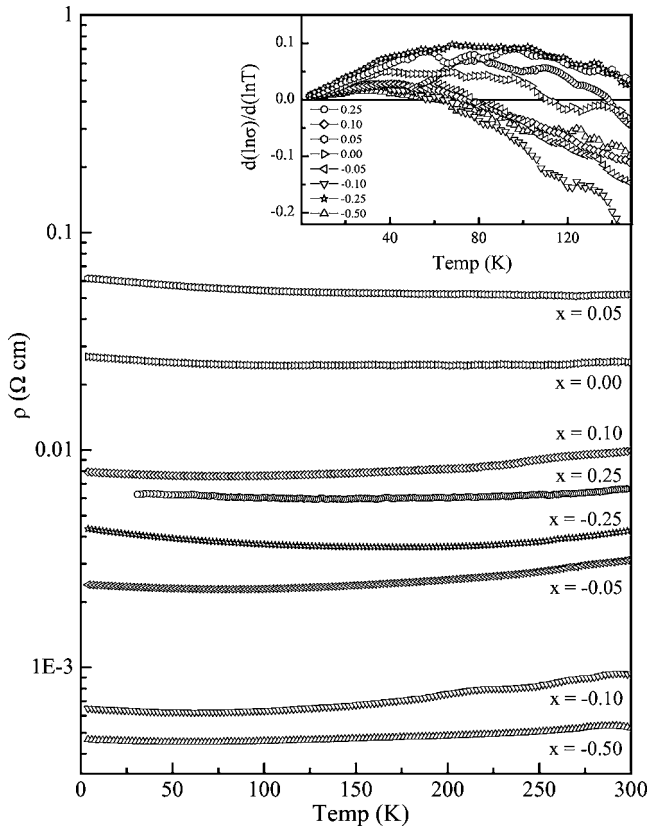


FIG. 2. Temperature dependence of the resistivity for various compositions in $\text{Sr}_2\text{Fe}_{1+x}\text{Mo}_{1-x}\text{O}_6$. The inset shows plots of $d(\ln \sigma)/d(\ln T)$ as a function of T .

$\rho(T)$ with decreasing temperature most probably arises from granular nature of the samples and due to the presence of disorder, instead of signaling an insulating ground state. This is further confirmed by plotting the $d(\ln \sigma)/d(\ln T)$ as a function of T in the inset to Fig. 2. The fact that this quantity approaches zero for all the compositions, instead of a finite value, as T approaches zero clearly suggests a metallic ground state for all the samples investigated here.

The inset to Fig. 3 shows the temperature dependence of magnetization for an applied field of $\mu_0 H = 0.1$ T. It is evident from these plots that all the samples are ferromagnetic, exhibiting a strong dependence of the transition temperature²⁰ T_c on the composition x . T_c 's (Fig. 3) exhibit a nearly linear increase with x between -0.5 and 0.05 and a very slow increase or near saturation for larger- x compositions. We can understand the monotonic increase of T_c with x in the $x \leq 0$ regime in terms of the increasing gain in kinetic energy concomitant with increasing spin polarization of itinerant electrons in the *ferromagnetic* Fe background, arising from the increasing concentration of Fe and a decreasing Fe-Fe separation. Considering an idealized, fully ordered structure with alternating Fe and Mo along the three cubic axes, all Fe ions substituting Mo beyond $x=0$ must necessarily give rise to Fe-O-Fe-O-Fe sequences. Strong superexchange interactions between Fe-O-Fe bonds should enhance the ferromagnetic coupling between Fe ions in the same sublattice, therefore increasing T_c as obtained in the case of a small extent of mis-site disorder.²¹ On the other hand, the

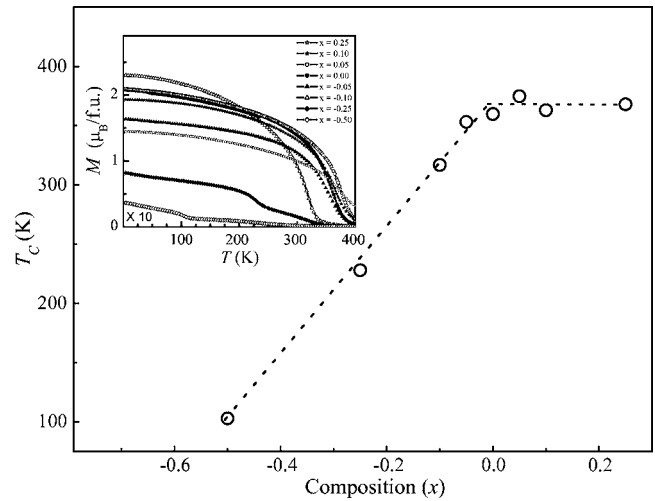


FIG. 3. Plot of T_c vs x . The dotted line is a guide to the eye. The inset shows the temperature dependence of magnetization for an applied field of $\mu_0 H = 0.1$ T, for various compositions.

decreasing number of itinerant electrons ($1-3x$) should lower T_c . As a result of these two opposing influences, T_c shows a near saturation close to $x=0$.

The inset to Fig. 4 shows the field dependence of the magnetization at 4.2 K. All the magnetization curves are qualitatively similar, establishing a soft ferromagnetic ground state for all the compositions. However, there is evidently a marked variation in the magnetic moment with the composition x . We have plotted the saturation magnetization per formula unit (f.u.) at 5 T for all the samples as a function of x in the main frame of Fig. 4. The saturation magnetization M_s shows the remarkable behavior of first increasing nearly linearly with x up to $x=0$ and then decreasing once again linearly with x , as suggested by the linear fits (solid

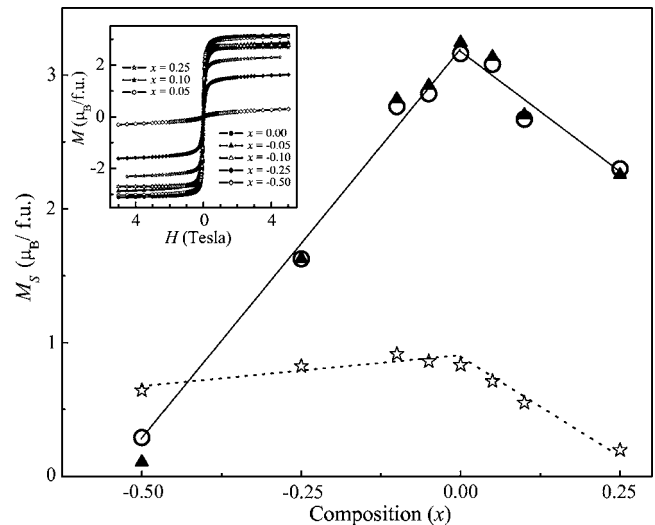


FIG. 4. Experimental saturation magnetization (open circle) at 4.2 K and 5 T as a function of the composition x compared with the calculated ones (solid triangle) based on the model presented in the text. Stars represent the calculated moment contribution from the conduction electrons per formula unit. The inset shows $M(H)$ at 4.2 K for various x .

lines) through the experimental data (open circle). This dependence, as we next show, severely restricts the available models to explain the magnetic structure, thereby providing a detailed understanding of magnetism and the role of antisite defects in this family of compounds.

We consider a strongly correlated description for Fe with the nominal configuration $3d^5$ forming high-spin $S=5/2$ localized spins and Mo^{6+} cores. The additional $1-3x$ nominally Mo electrons are itinerant, consistent with all compounds studied here being metallic. All five Fe d orbitals of one spin channel being occupied, itinerant electrons can hop to Fe sites only with an antiparallel orientation with respect to the localized spins; thus, the hopping stabilization of itinerant electrons also leads to its spin polarization in the idealized, fully ordered $\text{Sr}_2\text{FeMoO}_6$.^{3-5,21} It is also clear from this discussion that the polarization of each Mo site depends on the immediate Fe environment and its localized spin structure in the real system with antisite disorders.²¹ In the $x=0$ fully ordered case, Fe-Mo hopping gives rise to the minority band and half-metallic ground state.³⁻⁵ A qualitative understanding of the observed variation of the magnetic moment can be obtained easily. For the $x \leq 0$ regime, the saturation magnetization M_s increases with x primarily because the number of local moments increases and all Fe moments are ferromagnetically coupled. In the regime $x \geq 0$, as the Fe content increases, we find a rapid decrease of M_s . This is readily understood in terms of the additional Fe being necessarily connected to the next Fe by 180° Fe-O-Fe bonds and, consequently, being antiferromagnetically coupled. However, a more detailed and quantitative understanding requires separating two contributions to the M_s : namely, those (M_{Fe}) from localized moments of Fe and those (M_{Mo}) from conduction electrons. The local moment contribution, $M_{Fe} = 5(n_{Fe}^1 - n_{Fe}^2)$ with n_{Fe}^1 and n_{Fe}^2 being the proportion of Fe on sublattice 1 and 2, belonging to Fe and Mo, respectively, in the fully ordered $\text{Sr}_2\text{FeMoO}_6$. We define the order parameter a as the probability to find the minority component in its proper position. Therefore, the number of Fe atoms in the right position for $x \leq 0$, $n_{Fe}^1 = a(1+x)$, and, consequently, $n_{Fe}^2 = (1-a)(1+x)$, as well as $n_{Mo}^1 = 1-a(1+x)$ and $n_{Mo}^2 = a(1+x) - x$. Similarly in the case $x \geq 0$ the corresponding number for Mo is $n_{Mo}^2 = a(1-x)$ and $n_{Mo}^1 = (1-a)(1-x)$, with $n_{Fe}^2 = 1-a(1-x)$ and $n_{Fe}^1 = x+a(1-x)$. Therefore, we get $M_{Fe} = 5(2a-1)(1+x)$ for $x \leq 0$ and $5(2a-1)(1-x)$ for $x \geq 0$. We have determined the degree of order, a , in all our samples using Rietveld refinement as 0.65, 0.83, 0.92, 0.89, 0.91, 0.90, 0.86, and 0.83 for $x = -0.5, -0.25, -0.1, -0.05, 0.0, 0.05, 0.1$, and 0.25, respectively, completely determining the local moment contribution to the total moment. In order to estimate now the contribution of the conduction electron to M_s , we first note that the number of conduction electrons per Mo will vary as $n = (1-3x)/(1-x)$ in $\text{Sr}_2\text{Fe}_{1+x}\text{Mo}_{1-x}\text{O}_6$, in view of Fe retaining its localized trivalent state. In order to estimate the polarization M_{Mo} of the n conduction electrons, we

first note that Mo surrounded by six Fe atoms as in ordered $\text{Sr}_2\text{FeMoO}_6$ ($a=1$ and $x=0$) yields a fully polarized conduction band, leading to $M_{Mo} = -1\mu_B$ per f.u. The presence of Mo in the Fe sublattice, either due to disorder or due to Mo excess in the $x \leq 0$ regime, opens up Mo^1 - Mo^2 hopping channels *via* oxygen states, as in the end member SrMoO_3 , thereby depolarizing the conduction band. Simple Green function calculations in presence of disorder²² support this view. In the limit of SrMoO_3 ($x=-1$) with Mo surrounded only by Mo, the conduction moment is zero. Interpolating linearly between these two limits, by assuming the depolarization of the Mo electrons to be proportional to the number of Mo sites, in the other sublattice, we can write $M_{Mo} = -[n_{Mo}^1 + n_{Mo}^2 - 2n_{Mo}^1 n_{Mo}^2](1-3x)/(1-x)$, with the overall negative sign on M_{Mo} representing the antiferromagnetic coupling between M_{Fe} and M_{Mo} . The total magnetic moment per formula unit, $M_s = M_{Fe} + M_{Mo}$, is then readily evaluated as a function of only the composition x along with experimentally determined values of a , the order parameter. We have plotted these estimated $M_s(x)$ with closed triangles in the main frame of Fig. 4. Considering that the expression for M_s is fixed by x , with no adjustable parameter in the model, the agreement between the experimental and model results is exceptionally good. In the same figure, we have also shown the variation in the moment M_{Mo} arising from the conduction band (star) with composition x . Considering that the conduction states are only nominally Mo states with nearly equal contributions from Mo, Fe, and O (Ref. 10), we anticipate a moment of about one-third of M_{Mo} to be associated with the Mo sites, leading to about $-0.28\mu_B$ for the Mo sites in the $x=0$ compound in the present case. This is consistent with the estimates of Mo moment in $\text{Sr}_2\text{FeMoO}_6$.^{23,24}

IV. CONCLUSION

We have synthesized the solid solution $\text{Sr}_2\text{Fe}_{1+x}\text{Mo}_{1-x}\text{O}_6$ over a wide range of compositions. X-ray diffraction results establish a formal trivalent Fe^{3+} state over the entire range of x with the charge neutrality being maintained by a continuous changing of Mo valency. An analysis of the magnetic moment as a function of x supports a very specific model, where any Fe at the “wrong” crystallographic site is coupled antiparallel to the Fe moments at the correct site. Additionally, Mo is found to depolarize to an extent proportional to the number of Mo sites in the near-neighbor coordination shell. These results resolve the conflicting views proposed earlier concerning the magnetic structure of such double perovskite oxides.

ACKNOWLEDGMENTS

This project is supported by the Department of Science and Technology and Board of Research in Nuclear Sciences, Government of India.

*Also at Jawaharlal Nehru Centre for Advanced Scientific Research, Bangalore 560064, India. Electronic address: sarma@sscu.iisc.ernet.in

†Present address: Material Science and Technology Laboratory, Fuji Electric Advanced Technology, Tokyo 191-8502, Japan.

¹See, for example, *Colossal Magnetoresistive Oxides*, edited by Y. Tokura (Gordon and Breach, Amsterdam, 2000).

²K.-I. Kobayashi, T. Kimura, H. Sawada, K. Terakura, and Y. Tokura, *Nature (London)* **395**, 677 (1998).

³D. D. Sarma, P. Mahadevan, T. Saha-Dasgupta, S. Ray, and A. Kumar, *Phys. Rev. Lett.* **85**, 2549 (2000).

⁴J. Kanamori and K. Terakura, *J. Phys. Soc. Jpn.* **70**, 1433 (2001).

⁵D. D. Sarma, *Curr. Opin. Solid State Mater. Sci.* **5**, 261 (2001).

⁶Priya Mahadevan, Alex Zunger, and D. D. Sarma, *Phys. Rev. Lett.* **93**, 177201 (2004).

⁷Y. Tomioka, T. Okuda, Y. Okimoto, R. Kumai, K. I. Kobayashi, and Y. Tokura, *Phys. Rev. B* **61**, 422 (2000).

⁸S. Ray, A. Kumar, S. Majumdar, E. V. Sampathkumaran, and D. D. Sarma, *J. Phys.: Condens. Matter* **13**, 607 (2001).

⁹A. S. Ogale, R. Ramesh, and T. Venkatesan, *Appl. Phys. Lett.* **75**, 537 (1999).

¹⁰T. Saha-Dasgupta and D. D. Sarma, *Phys. Rev. B* **64**, 064408 (2001).

¹¹D. D. Sarma, Sugata Ray, K. Tanaka, and A. Fujimori, cond-mat/0311013 (unpublished).

¹²M. García-Hernández, J. L. Martínez, M. J. Martínez-Lope, M. T. Casais, and J. A. Alonso, *Phys. Rev. Lett.* **86**, 2443 (2001).

¹³D. D. Sarma, E. V. Sampathkumaran, S. Ray, R. Nagarajan, S. Majumdar, A. Kumar, G. Nalini, and T. N. Guru Row, *Solid State Commun.* **114**, 465 (2000).

¹⁴L. I. Balcells, J. Navarro, M. Bibes, A. Roig, B. Martinez, and J. Fontcuberta, *Appl. Phys. Lett.* **78**, 781 (2001).

¹⁵J. Navarro, L. I. Balcells, F. Sandiumenge, M. Bibes, A. Roig, B. Martinez, and J. Fontcuberta, *J. Phys.: Condens. Matter* **13**,

8481 (2001).

¹⁶D. Sánchez, M. Garcíndez, J. L. Martínez, J. A. Alonso, M. J. Martínez-Lope, M. T. Casais, and A. Møllergård, *J. Magn. Mater.* **242**, 729 (2002).

¹⁷T. Takeda, R. Kanno, Y. Kawamoto, M. Takano, S. Kawasaki, T. Kamiyama, and F. Izumi, *Solid State Sci.* **2**, 673 (2000).

¹⁸Unpublished Mössbauer spectra of these samples clearly support this view.

¹⁹G. Y. Liu, G. H. Rao, X. M. Feng, H. F. Yang, Z. W. Ouyang, W. F. Liu, and J. K. Liang, *Physica B* **334**, 229 (2003); G. Y. Liu, G. H. Rao, X. M. Feng, H. F. Yang, Z. W. Ouyang, W. F. Liu, and J. K. Liang, *J. Alloys Compd.* **353**, 42 (2003); G. Y. Liu, G. H. Rao, X. M. Feng, H. F. Yang, Z. W. Ouyang, W. F. Liu, and J. K. Liang, *J. Phys.: Condens. Matter* **15**, 2053 (2003).

²⁰We estimate T_c by the peak in the derivative curve, dM/dT ; the usual definition of T_c by the temperature where $M(T)$ begins to rise rapidly would yield transition temperatures that are typically higher than the present estimates. The two lowest- x compositions suggest the presence of low concentrations of magnetically impure phases by the smooth distribution of finite M at higher temperatures, though the main compositions clearly show sharp variations in $M(T)$ defining T_c .

²¹R. Allub, O. Navarro, M. Avignon, and B. Alascio, *Physica B* **320**, 13 (2002); E. Carvajal, O. Navarro, R. Allub, M. Avignon, and B. Alascio, *J. Magn. Mater.* **273**, 1774 (2004); E. Carvajal, O. Navarro, R. Allub, M. Avignon, and B. Alascio, *Eur. Phys. J. B* **48**, 179 (2005).

²²R. Allub, B. Alascio, and M. Avignon (unpublished).

²³S. Ray, A. Kumar, D. D. Sarma, R. Cimino, S. Turchini, S. Zennaro, and N. Zema, *Phys. Rev. Lett.* **87**, 097204 (2001).

²⁴M. Besse, V. Cros, A. Barthèlèmy, H. Jaffrés, J. Vogel, F. Petroff, A. Mirone, A. Tagliaferri, P. Bencok, P. Decorse, P. Berthet, Z. Szotek, W. M. Temmerman, S. S. Dhesi, N. B. Brookes, A. Rogalev, and A. Fert, *Europhys. Lett.* **60**, 608 (2002).